Available online at www.sciencedirect.com
SCIENCE DIRECT®
Journal of Sound and Vibration 281 (2005) 1–20
JOURNAL OF SOUND AND VIBRATION
www.elsevier.com/locate/jsvi

Gantry cranes gain scheduling feedback control with friction compensation

Hanafy M. Omar[a], Ali H. Nayfeh[b,*]

[a]*Aerospace Engineering Department, King Fahd University of Petroleum and Minerals, P.O. Box 1794, Dhahran 31261, Saudi Arabia*
[b]*Department of Engineering Science and Mechanics, MC 0219, Virginia Polytechnic Institute and State University, Blacksburg, VA 24061, USA*

Received 27 August 2002; accepted 6 January 2004
Available online 15 September 2004

Abstract

We designed a controller based on gain-scheduling feedback to move a load on a gantry crane from point to point within one oscillation cycle and without inducing large swings. The settling time of the system is taken to be equal to the period of oscillation of the load. This criterion enables calculation of the controller feedback gains for varying load weight and cable length. Numerical simulations show that the controller is effective in reducing load oscillations and transferring the load in a reasonable time compared with that of optimal control.

To experimentally validate the theory, we had to compensate for friction. To this end, we estimated the friction, and then applied an opposite control action to cancel it. To estimate the friction force, we assumed a mathematical model, and then we estimated the model coefficients using an off-line identification technique, such as the method of least squares (LS). First, the process of identification is applied to a theoretical model of a DC motor with known friction coefficients. From this example, some guidelines and rules are deduced for the choice of the LS parameters. Then, the friction coefficients of the gantry crane model are estimated and validated.

*Corresponding author. Tel.: +1-540-231-5453; fax: +1-540-231-2290.
E-mail addresses: hmomar@kfupm.edu.sa (H.M. Omar), anayfeh@vt.edu (A.H. Nayfeh).

0022-460X/$ - see front matter © 2004 Elsevier Ltd. All rights reserved.
doi:10.1016/j.jsv.2004.01.037

1. Introduction

Gantry cranes are widely used to transport heavy loads and hazardous materials in factories and nuclear installations. They consist of a trolley, which translates in a horizontal plane. The payload is attached to the trolley by a cable, whose length can be varied by a hoisting mechanism. The load with the cable is treated as a one-dimensional pendulum with one-degree-of-freedom sway.

The objective of crane operation is to move a load from point to point in the minimum time such that the load reaches its destination without swinging. Usually a skillful operator is responsible for this task. During the operation, the load is free to swing in a pendulum-like motion. If the swing exceeds a proper limit, it must be damped or the operation must be stopped until the swing dies out. Either option consumes time, which reduces the facility availability. These problems have motivated many researchers to develop control algorithms to automate crane operations. However, most of the existing schemes are not suitable for practical implementation. Therefore, most industrial cranes are not automated and still depend on operators, who sometimes fail to compensate for the swing. This failure may subject the load and the environment to danger. Another difficulty of crane automation is the nature of the crane environment, which is often unstructured in shipyards and factory floors. The control algorithm should be able to cope with these conditions.

1.1. Cranes automation approaches

The operation of cranes can be divided into five steps: gripping, lifting, moving the load from point to point, lowering, and ungripping. A full automation of these processes is possible, and some research has been directed towards that task [1]. Moving the load from point to point is the most time-consuming task in the process and requires a skillful operator to accomplish it. Suitable methods to facilitate moving loads without inducing large swings are the focus of much current research. We can divide crane automation into two approaches. In the first approach, the operator is kept in the loop and the dynamics of the load are modified to make his job easier. One way is to add damping by feeding back the load swing angle and its rate or by feeding back a delayed version of the swing angle [2]. This feedback adds an extra trajectory to that generated by the operator. A second way is to avoid exciting the load near its natural frequency by adding a filter to remove this frequency from the input [3]. This introduces a time delay between the operator action and the input to the crane. This delay may confuse the operator. A third way is to add a mechanical absorber to the structure of the crane [4]. Implementing this method requires a considerable amount of power. We have to mention that the algorithms in Refs. [4,2] are developed for controlling the swing in the ship-mounted cranes. However, these algorithms can be applied to the gantry cranes which are mounted on a fixed platform.

In the second approach, the operator is removed from the loop and the operation is completely automated. This can be done using various techniques. The first is based on generating trajectories to transfer the load to its destination with minimum swing. These trajectories are obtained by input shaping or optimal control techniques. A second technique is based on the feedback of the position and the swing angle. A third technique is based on dividing the controller design problem

into two parts: an anti-swing controller and a tracking controller. Each one is designed separately and then combined to ensure the performance and stability of the overall system.

Since the swing of the load is affected by the acceleration of the motion, many researchers have concentrated on generating trajectories, which deliver the load in the shortest possible time and at the same time minimize the swing. These trajectories are obtained generally by using optimization techniques. The objective function can be the transfer time [5], the control action [6], or the swing angle [7]. Another important method of generating trajectories is input shaping, which consists of a sequence of acceleration pulses. These sequences are generated such that there is no residual swing at the end of the transfer operation [8–10]. The resulting controller is open loop, which makes it sensitive to external disturbances and to parameter variations. In addition, the required control action is bang–bang, which is discontinuous. Moreover, it usually requires a zero-swing angle at the beginning of the process, which cannot be realized practically. To avoid the open-loop disadvantages, many researchers [11,12] have investigated optimal control through feedback. They found that optimal control performs poorly when implemented in a closed-loop form. The poor performance is attributed to limit cycles resulting from the oscillation of the control action around the switching surfaces.

Feedback control is well-known to be less sensitive to disturbances and parameter variations. Hence, it is an attractive method for crane control design. Ridout [13] developed a controller, which feeds back the trolley position and speed and the load swing angle. The feedback gains are calculated by trial and error based on the root-locus technique. Later, he improved his controller by changing the trolley-velocity gain according to the error signal [14]. Through this approach, the system damping can be changed during transfer of the load. Initially, damping is reduced to increase the velocity, and then it is increased gradually. Consequently, a faster transfer time is achieved. However, the nominal feedback gains are obtained by trial and error. This makes the process cumbersome for a wide range of operating conditions. Salminen [15] employed feedback control with adaptive gains, which are calculated based on the pole-placement technique. Since the gains are fixed during the transfer operation, his control algorithm can be best described as gain scheduling rather than adaptation. Hazlerigg [16] developed a compensator with its zeros designed to cancel the dynamics of the pendulum. This controller was tested on a physical crane model. It produced good results except that the system was underdamped. Therefore, the system response was oscillatory, which implies a longer transfer time. Hurteau and Desantis [17] developed a linear feedback controller using full-state feedback. The controller gains are tuned according to the cable length. However, if the cable length changes in an unqualified way, degradation of the system performance occurs. In addition, the tuning algorithm was not tested experimentally.

As mentioned before, the objective of the crane control is to move the load from point to point and at the same time minimize the load swing. Usually, the controller is designed to achieve these two tasks simultaneously, as in the aforementioned controllers. However, in another approach used extensively, the two tasks are treated separately by designing two feedback controllers. The first one is an anti-swing controller. It controls the swing damping by a proper feedback of the swing angle and its rate. The second is a tracking controller designed to make the trolley follow a reference trajectory. The trolley position and velocity are used for tracking feedback. The position trajectory is generally the classical velocity pattern, which is obtained from open loop optimal control or input shaping techniques. The tracking controller can be a classical

proportional-derivative (PD) controller [2] or a fuzzy logic controller (FLC) [18–22]. Similarly, the anti-swing controller is designed by different methods. Masoud et al. [2] used a delayed feedback, whereas Nalley and Trabia [19], Yang et al. [18], and Al-Mousa [22] used FLC. Separation of the control tasks, anti-swing and tracking, enables the designer to handle different trajectories according to the work environment. Generally, the cable length is considered in the design of the anti-swing controller. However, the effect of the load mass is neglected in the design of the tracking controller. The system response is slow compared with that of optimal control.

Raising the load during transfer (hoisting) is needed only to avoid obstacles. This motion is slow, and hence variations in the cable length can be considered as a disturbance to the system. Then, the effect of variations in the cable length is investigated through simulation to make sure that the performance does not deteriorate. However, there are few studies that include hoisting in the design of controllers [23]. At this stage of work, we do not include the hoisting in the controller design.

The effect of the load weight on the dynamics is usually ignored. However, Lee [24] and Omar and Nayfeh [25] consider it in the design of controllers for gantry and tower cranes, respectively. From these studies, we find that for very heavy loads compared to the trolley weight, the system performance deteriorates if the load weight is not included in the controller design.

1.2. Experiment setup

To validate the designed controllers, we built a crane model as shown in Fig. 1. The control algorithms are implemented on a PC using C++. An interface board (IB) is used to link the computer with the crane system, as shown in the experimental setup diagram in Fig. 2. The crane

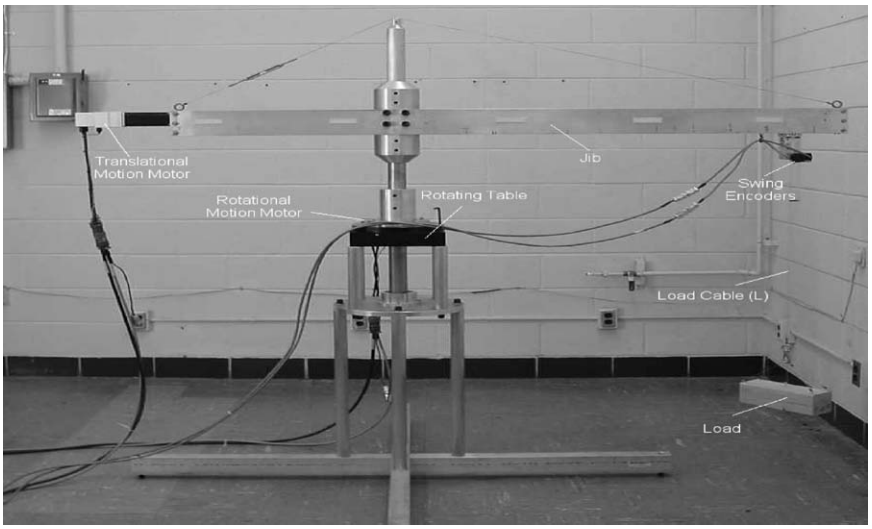

Fig. 1. Crane model used in the experiment.

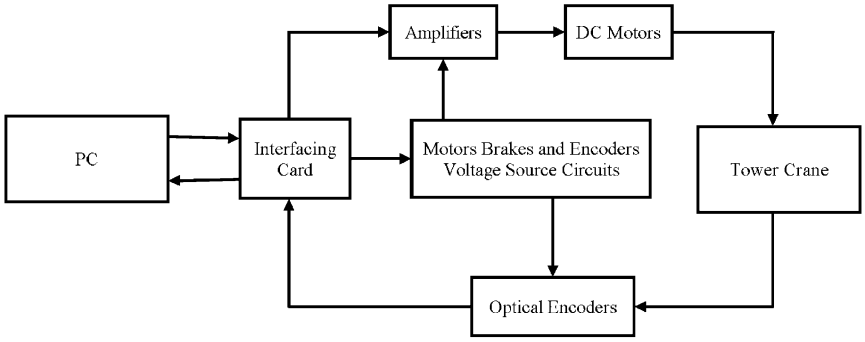

Fig. 2. Experimental setup diagram.

is composed of a trolley assembly moving horizontally on a leadscrew, which is driven by a brushless servomotor. The leadscrew has a pitch $p = 0.5\,\text{in/rev}$. A servomotor drives the leadscrew. The motor has an optical encoder with a resolution of 2000 lines/rev. This encoder measures the motor positions, which in turn are sent to the IB. The motor is equipped with an internal brake, which is engaged when the power is disabled. This brake requires a 24 V for opening. The load-swing angle is measured by an optical encoder with a resolution of 6000 lines/rev. Five volt signals are used to feed the swing encoder. This encoder is connected to digital counters built in the IB; the result is sent to the PC. The output signals of the encoders are the feedback signals of the system. According to these signals, the control algorithm calculates the proper control action. This action is sent to the motor. Because the motor requires high power for operating, it is connected to an amplifier. The amplifier serves as a communication unit between its motor and the IB.

In this setup, we observed the following:

- The leadscrew-nut mechanism generates a high amount of friction.
- The performance of the trolley depends on the motion direction.
- When a filtered velocity is used in the control-action calculation, the motion in the positive direction becomes oscillatory with high magnitude. However, when unfiltered data are used, the motion becomes smoother, even with the noise introduced by the numerical differentiation. This behavior may be a result of the interaction between the friction and the delay introduced by the filter. For this reason, the unfiltered velocity is used to determine the control action sent to the trolley motor.

1.3. Friction compensation

Friction within mechanical systems is unavoidable. In our experiment, most of the friction is generated from the leadscrew-nut mechanism which drives the trolley. The friction characteristics of rigid bodies moving relative to each other at substantial speed are fairly linear. When the bodies in contact are at rest, there is an opposing frictional force equal to the applied force on the bodies. This sticking force will prevent motion until the applied force exceeds the maximum stiction level

inherent between the materials in contact. It has been experimentally determined that immediately after motion occurs, friction decreases rapidly in magnitude until it reaches a critical value (Stribeck effect) after which it increases linearly with velocity. Moreover, friction has nonsymmetric characteristics, such as dependence of the position and motion direction. For a more comprehensive discussion of the phenomenological nature of friction, we refer the reader to Armstrong et al. [26] and Canudas et al. [27].

There are several methods to overcome friction effects. The first uses high-feedback-gain controllers, which may reduce the effect of the friction nonlinearities. However, this approach has severe limitations because the nonlinearities dominate any compensation for small errors. Limit cycles may appear as a consequence of the dynamic interaction between the friction forces and the controller, especially when the controller contains integral terms. The second uses high-frequency bias signal injection. Although it may alleviate friction effects, it may also excite high-frequency harmonics in the system. The third uses friction compensation, which aims to remove the effect of friction completely.

The third method has an advantage over the other methods because the system becomes linear after compensation. Thus, control algorithms based on the linear model can be applied directly. The compensation is done by estimating the friction of the system, and then applying an opposite control action to cancel it. The compensation can be done on-line to track the friction variations, which may occur due to changes in the environment and mechanical wear. Many researchers developed adaptive friction compensation for various applications using different adaptation techniques and models [28,29]. However, to obtain a good estimate of the friction using the adaptive approach, one needs to persistently excite the system [30]. In our system, the input signals do not have this characteristic. Moreover, the friction can be assumed to be constant during the operation without affecting the system performance. This enables us to estimate the friction off-line using an appropriate persistent excitation.

The estimation process requires a model of friction. Friction models have been extensively discussed in the literature [26,31]. It is well established that friction is a function of the velocity; however, there is disagreement about the relationship between them. Among these models, we choose the one proposed by Canudas et al. [28] because of its simplicity and because it represents most of the friction phenomena. This model consists of constant viscous and Coulomb terms. These constants change with the motion direction.

1.4. Objective

The main objective of this work is to design robust, fast, and practical controllers for gantry cranes to transfer the load from point to point in a short time as fast as possible and, at the same time keep the load swing small during the transfer process and completely eliminate it at the load destination. Moreover, variations of the system parameters, such as the cable length and the load weight, are taken into account. Practical considerations, such as the control action power, maximum acceleration, and velocity, are also taken into account. In addition, friction effects are included in the design using a friction compensation technique.

2. Modeling of gantry cranes

We use the Lagrangian approach to derive the equations of motion. It follows from Fig. 3 that the load and trolley position vectors are given by

$$\mathbf{r}_L = \{x + L\sin(\phi),\ -L\cos(\phi)\} \quad \text{and} \quad \mathbf{r}_T = \{x, 0\}. \tag{1}$$

Then, the kinetic and potential energies of the whole system are given by

$$T = \tfrac{1}{2}m\,\mathbf{r}_L \cdot \mathbf{r}_L + \tfrac{1}{2}M\,\mathbf{r}_T \cdot \mathbf{r}_T, \tag{2}$$

$$V = -mgL\cos(\phi). \tag{3}$$

Let the generalized forces corresponding to the generalized displacements $\mathbf{q} = \{x, \phi\}$ be $\vec{F} = \{F_x, 0\}$. Constructing the Lagrangian $\mathscr{L} = T - V$ and using Lagrange's equations

$$\frac{\mathrm{d}}{\mathrm{d}t}\left(\frac{\partial \mathscr{L}}{\partial \dot{q}_j}\right) - \frac{\partial \mathscr{L}}{\partial q_j} = F_j, \quad j = 1, 2, \tag{4}$$

we obtain the following equations of motion:

$$(m + M)\,\ddot{x} + mL\ddot{\phi}\cos(\phi) + m\ddot{L}\sin(\phi) + 2m\dot{L}\dot{\phi}\cos(\phi) - mL\dot{\phi}^2\sin(\phi) = F_x, \tag{5}$$

$$L\ddot{\phi} + g\sin(\phi) + 2\dot{L}\dot{\phi} + \ddot{x}\cos(\phi) = 0. \tag{6}$$

For safe operation, the swing angle should be kept small. In this study, we assume that changing the cable length is needed only to avoid obstacles in the path of the load. This change can also be considered small. Using these two assumptions and dividing Eq. (5) by M, we reduce the equations of motion to

$$\ddot{x} - m_t g\phi = \bar{F}_x, \tag{7}$$

$$L\ddot{\phi} + g\phi + \ddot{x} = 0, \tag{8}$$

where

$$m_t = \frac{m}{M}, \quad \bar{F}_x = \frac{F_x}{M}. \tag{9}$$

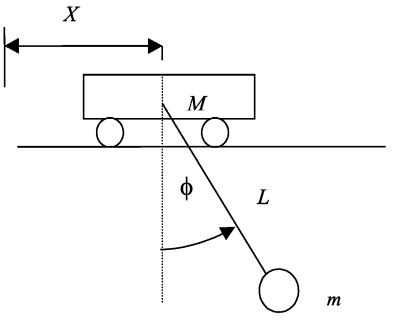

Fig. 3. Gantry-crane model.

Because the motor has a small time constant relative to the mechanical system, the force exerted by it can be considered as a constant gain and expressed as

$$\bar{F}_x = K_{mx} V_x, \tag{10}$$

where V_x is the input voltage to the motor.

3. Friction estimation and compensation

The friction model in Fig. 4 can be expressed in the form

$$F_f = (c_+ - b_+\dot{x})\eta + (-c_- - b_-\dot{x})\xi + F_{fs}(1-\eta)(1-\xi), \tag{11}$$

where c and b are the Coulomb and viscous friction coefficients, respectively, the positive and minus signs refer to the positive and negative directions of the velocity, and F_{fs} is the stiction friction at zero velocity. The stiction friction theoretically appears at zero velocity. It opposes the motion until the control action exceeds it. It also depends on the direction of the motion. To cancel it, we need to reverse the control action after it passes zero velocity, which generates limit cycles. Consequently, the system response becomes oscillatory and the response is unacceptable. To avoid this problem, we assume the stiction to be a continuous function of the control action with a sharp slope in the form

$$F_{fs} = f_{sh} + f_s \tanh(A\,V), \tag{12}$$

where f_s and A are the magnitude and slope of the friction. A shift f_{sh} is introduced to account for asymmetric characteristics of the friction. Due to the error resulting from the numerical computation and differentiation, the zero velocity should be defined as a region instead of a crisp

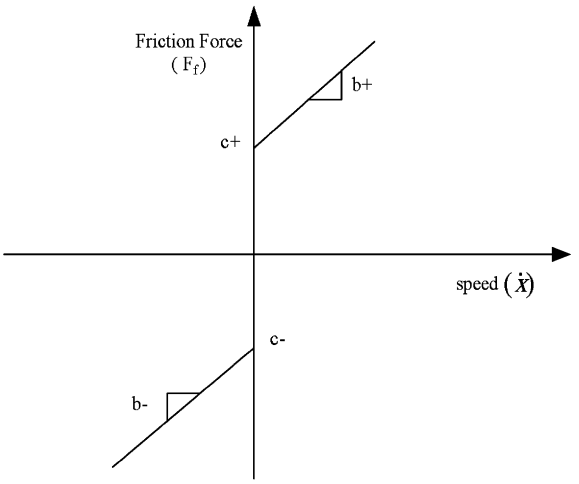

Fig. 4. Friction model.

value. Therefore, we introduce the parameters ξ and η defined as

$$\xi = 0,\ \eta = 0,\ |\dot{x}| < d_s, \quad \xi = 0,\ \eta = 1,\ \dot{x} > d_s, \quad \xi = 1,\ \eta = 0,\ \dot{x} < -d_s, \tag{13}$$

where d_s is the upper limit of the zero-velocity region.

The Coulomb and viscous friction coefficients are determined using the method of least squares, while the stiction friction parameters are determined experimentally to be equal to the control action at which the motor starts to move. Then, the estimated friction force F_f is added to the control action to linearize the model as follows:

$$\ddot{x} = K_m(u - F_f/K_m) \rightarrow \ddot{x} = K_m V, \tag{14}$$

where V is the control action determined from the linear model. The actual control action is

$$u = V + F_f/K_m, \tag{15}$$

where K_m is the motor constant, which is a known parameter.

The translational and rotational motions outside the zero-velocity region, without stiction friction, can be represented by

$$\ddot{x} + b\dot{x} = K_m u - c_+\eta + c_-\xi. \tag{16}$$

Without affecting the friction model, we denote the viscous friction coefficient by b for both directions. Using this notation, we write the linear model of Eq. (16) as

$$\ddot{x} + b\dot{x} = K_m u. \tag{17}$$

The discrete form of this linear system with a sampling period T_s and a zero order hold is

$$\frac{X(z)}{V(z)} = \frac{a_1 z + a_2}{(z-1)(z-a)}, \tag{18}$$

where

$$a_1 = \frac{K_m}{b^2}(b\,T_s - 1 + \mathrm{e}^{-bT_s}), \quad a_2 = \frac{K_m}{b^2}(1 - \mathrm{e}^{-bT_s} - bT_s\mathrm{e}^{-bT_s}), \quad a = \mathrm{e}^{-bT_s}. \tag{19}$$

It is difficult to obtain a linear regression form using the above parameters. Assuming bT_s to be small and approximating e^{-bT_s} with $1 - bT_s$, we obtain $a_1 = 0$, $a_2 = K_m T^2$, and $a = 1 - bT_s$. Then, the simplified discrete form of Eq. (17) can be written as

$$[x(k) - 2x(k-1) + x(k-2)]/T_s^2 = -b[x(k-2) - x(k-1)]/T_s + K_m u(k-2). \tag{20}$$

We can put this discrete model in another form by defining the discrete acceleration and velocity as

$$\begin{aligned} \ddot{x}_d(k) &= [x(k) - 2x(k-1) + x(k-2)]/T_s^2, \\ \dot{x}_d(k) &= [x(k-2) - x(k-1)]/T_s. \end{aligned} \tag{21}$$

Then, the discrete form in Eq. (20) becomes

$$\ddot{x}_d(k) = -b\dot{x}_d(k) + K_m u(k-2). \tag{22}$$

Adding the Coulomb friction to the model and considering the viscous friction in both directions, we write the discrete model as

$$\ddot{x}_d(k) = -b_+\dot{x}_d(k)\eta - b_-\dot{x}_d(k)\xi + K_m u(k-2) - c_+\eta + c_-\xi. \tag{23}$$

The regression form in matrix notation is

$$y(k) = \phi(k)\Theta, \tag{24}$$

where

$$y(k) = \frac{\ddot{x}_d(k)}{K_m} - u(k-2), \quad \phi(k) = \left[\dot{x}_d(k)\eta \; \dot{x}_d(k)\xi \; -\eta \; \xi\right], \quad \Theta = \left[\frac{b_+}{K_m} \quad \frac{b_-}{K_m} \quad \frac{c_+}{K_m} \quad \frac{c_-}{K_m}\right]^{\mathrm{T}}.$$

Using the method of least squares, we calculate the unknown parameters vector Θ from

$$\Theta = (\mathbf{Y}^{\mathrm{T}}\mathbf{Y})^{-1}\mathbf{Y}^{\mathrm{T}}\Phi, \tag{25}$$

where $\mathbf{Y} = [y(1)\ y(2)\ \cdots y(n)]$, $\Phi = [\phi(1)\ \phi(2)\ \cdots \phi(n)]$, and n is the number of samples.

To apply the estimation technique, we stabilize the system using a PD controller. Then, a PE reference is applied. The output is filtered and then used to estimate the unknown parameters using Eq. (25). First, the procedure is applied to a theoretical model with known parameter values to understand the effect of friction on the estimation. From this study, we obtain some guidelines for the real-system estimation. These guidelines are summarized as follows.

- Coulomb friction adds high frequencies to the system output. These frequencies should not be removed by filtering; otherwise, the estimated parameters will not be correct, especially the viscous friction coefficients. Therefore, the filter cut-off frequency should be chosen properly. It should be increased with Coulomb friction. At the same time, high frequencies resulting from the measurement and numerical differentiation should be removed. It was found that a cut-off frequency of $0.1f_s$ is a reasonable choice, where f_s is the sampling frequency.
- The acceleration and velocity are obtained by numerical differentiation, which introduces some errors, especially around zero velocity. Also, due to the discontinuity in the friction at the zero velocity, the acceleration is very high and oscillatory. This results in bad estimates of the friction coefficients. Therefore, the data in the zero-velocity region should be excluded to obtain a realistic estimation. The width of the zero-velocity region d_s is obtained by inspecting the velcoity time response.

4. Gain-scheduling adaptive feedback controller

We use state feedback to control the position of the trolley and at the same time reduce the load swing. We first propose a controller having the form

$$V_x = K(x_{rm} - K_x x - K_{\dot{x}}\dot{x} + K_\phi \phi). \tag{26}$$

Now, the question arises regarding how to adjust the gains in this controller to obtain the best performance for a wide range of cable lengths and loads. The main objective is to make the swing

angle as small as possible. The minimum number of load oscillations during which this can be achieved is one cycle. We note that, when the trolley response is critically damped, the load completes one cycle, which indicates that the settling time for the trolley should be equal to the period of the load. We use this criterion to choose the location of the closed-loop poles and hence the feedback gains [17]. The design procedure is described next.

To make the trolley response critically damped, we choose its poles to be repeated and equal to a. Because the load performance should be oscillatory, we choose its poles to be $-\zeta\omega_n \pm \omega_n\sqrt{1-\zeta^2}\mathrm{j}$. The final closed-loop characteristic equation is

$$(s+a)^2(s^2+2\zeta\omega_n s+\omega_n^2)=0. \tag{27}$$

From simulations, the best damping ratio that can be chosen is $\zeta = 1/\sqrt{2}$. Using the above-mentioned settling time criterion, we have

$$\frac{4}{a}=\frac{2\pi}{\sqrt{g/L}} \rightarrow a=\frac{4\sqrt{g/L}}{2\pi}. \tag{28}$$

Comparing the required closed-loop characteristic Eq. (27) with that of the system, we obtain the following four nonlinear algebraic equations:

$$\pi K K_{\dot{x}} K_{mx} - 8\sqrt{\frac{g}{L}} - 4\pi\xi\omega_n = 0, \tag{29}$$

$$2L\pi\omega_n\left(8\sqrt{\frac{g}{L}}\xi+\pi\omega_n\right)-\pi^2 K K_{mx}(L K_x+K_\phi)+8g-g\pi^2(2+m_t)=0, \tag{30}$$

$$8\pi\sqrt{\frac{g}{L}}L\omega_n^2 - g\pi^2 K K_{\dot{x}} K_{mx} + 16 g \xi \omega_n = 0, \tag{31}$$

$$8\omega_n^2 - \pi^2 K K_x K_{mx} = 0. \tag{32}$$

The steady-state error is given by $A(1-1/K_x)$, where A is the value of the step input to the system. For zero steady-state error, we let $K_x = 1$. Because K_{mx} is known and fixed, we end up with four equations in the four unknowns $(K, K_{\dot{x}}, K_\phi, \omega_n)$, which can be calculated symbolically as functions of (m_t, L). At this stage, there is no control over K, which is the dominant factor in determining the maximum acceleration of the trolley, especially at the beginning of the motion.

Because the acceleration increases as the error increases, for long travel distances, the motor acceleration required at the beginning will be very high, which is not realistic. Also, this acceleration increases as L decreases because it will be required to move the load to its target in a short time; this requires a high speed and consequently a large acceleration at the beginning of the process. To overcome this problem, we predetermine K not to exceed the maximum acceleration of the motor. Now, we end up with four equations in the four unknowns $(K_x, K_{\dot{x}}, K_\phi, \omega_n)$, which can be calculated as before as functions of (m_t, L, K). However, the steady-state error will not be zero. To make it zero, we add another gain. This leads

to the full-state feedback controller

$$v = K(x_{rm} - K_x x - K_{\dot{x}}\dot{x} + K_\phi \phi + K_{\dot{\phi}}\dot{\phi}). \tag{33}$$

Applying the characteristic Eq. (27) and comparing it with that of the system, we obtain four nonlinear equations, which are the same as Eqs. (29)–(32) except that there is an additional term $\pi K K_\tau K_{\dot{\phi}}$ in Eq. (29). By choosing $K_x = 1$ to obtain a zero steady-state error and choosing K not to exceed the maximum available control action, we determine $(K_{\dot{x}}, K_\phi, K_{\dot{\phi}}, \omega_n)$ as functions of the remaining parameters (m_t, L).

The stability of the system is governed by ω_n. For asymptotic stability, it should be positive, which is guaranteed when the gains are calculated.

4.1. Simulations

The full nonlinear equations of motion were used in the simulations with the following numerical values in SI units in meters and kilograms: $K_{mx} = 1.34$.

The time was scaled by the oscillation period of the load; that is, $\bar{t} = t/(2\pi/\sqrt{g/L}) = t/T$. This scaling makes the responses similar for all values of L.

Variation of the feedback gains with the cable length for $m_t = 0$ using the partial state-feedback controller is shown in Fig. 5. We note that K is inversely proportional to the cable length because the load natural frequency increases with the cable length, which decreases the system settling time and consequently increases K. Thus so, it is better to raise the load as much as possible to transfer it in a short time. However, the speed of the trolley should not exceed the motor maximum speed.

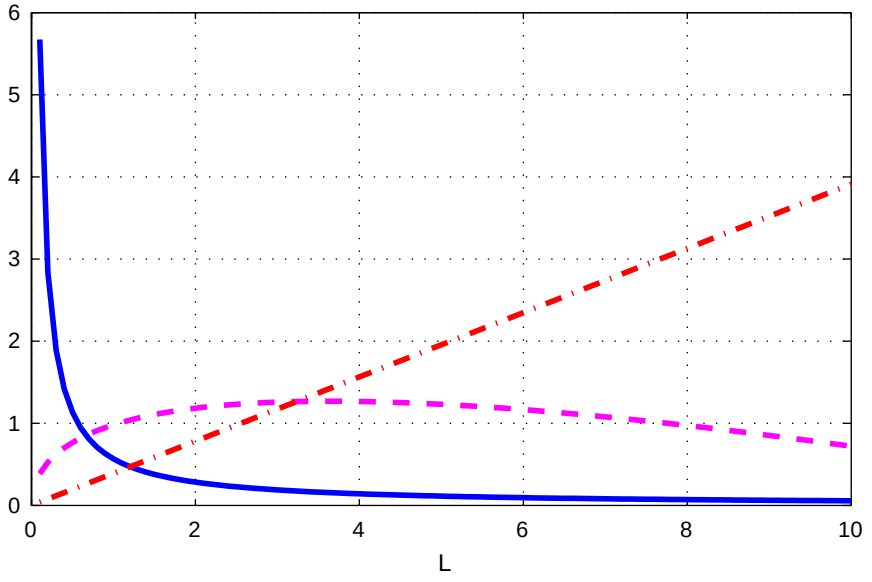

Fig. 5. Variation of the gains with the cable length using the partial-state feedback controller when $m_t = 0$: ——, $K/10$; - - -, $K_{\dot{x}}$; and - · - · - ·, $K_\phi/10$.

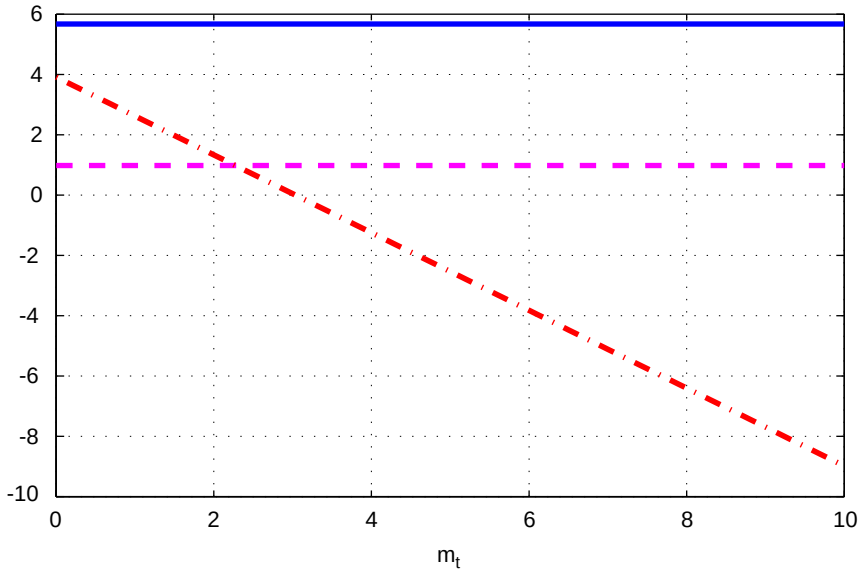

Fig. 6. Variation of the feedback gains with the load weight using the partial-state feedback controller when $L = 1$ m: ——, K; - - -, $K_{\dot{x}}$; - · - · - ·, K_{ϕ}.

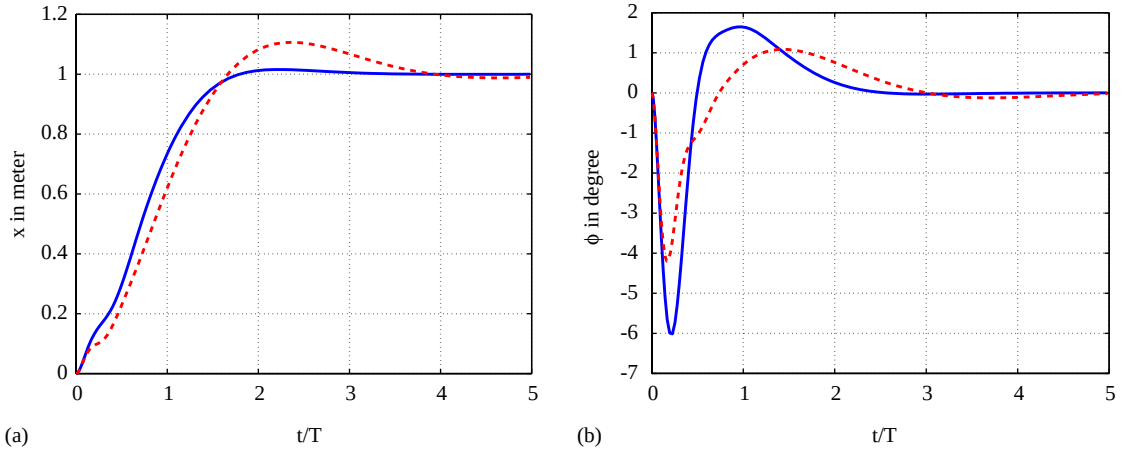

Fig. 7. Effect of changing the load mass on (a) the trolley position x and (b) the load swing angle ϕ when $m_t = 5$ and $L = 1$ m: ——, using the gains corresponding to $m_t = 5$; and - - -, using the gains corresponding to $m_t = 0$.

The swing-angle gain is linearly proportional to L. If the swing distance $L\phi$ was used in the feedback instead of ϕ, K_{ϕ} would be independent of L.

It follows from Fig. 6 that the swing-angle gain decreases linearly with m_t, whereas the other gains do not change. Examining Eq. (8), we note that $m_t g\phi$ can be considered as an extra force in

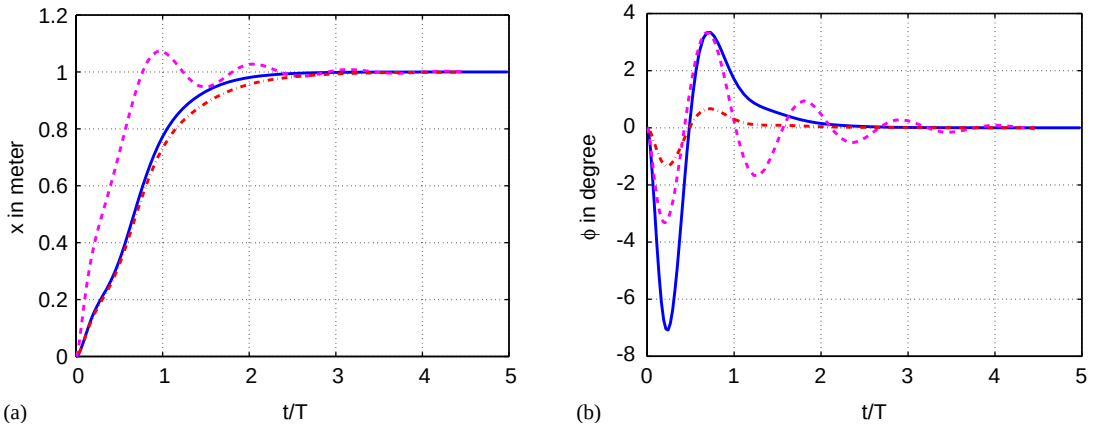

Fig. 8. Effect of changing the cable length on (a) the trolley position x and (b) the load swing angle using full-state feedback: ——, $L = 1$ m using the adapted gains; - - - -, $L = 5$ m using the gains corresponding to $L = 1$ m; and - · - · - · -, $L = 5$ m using the adapted gains.

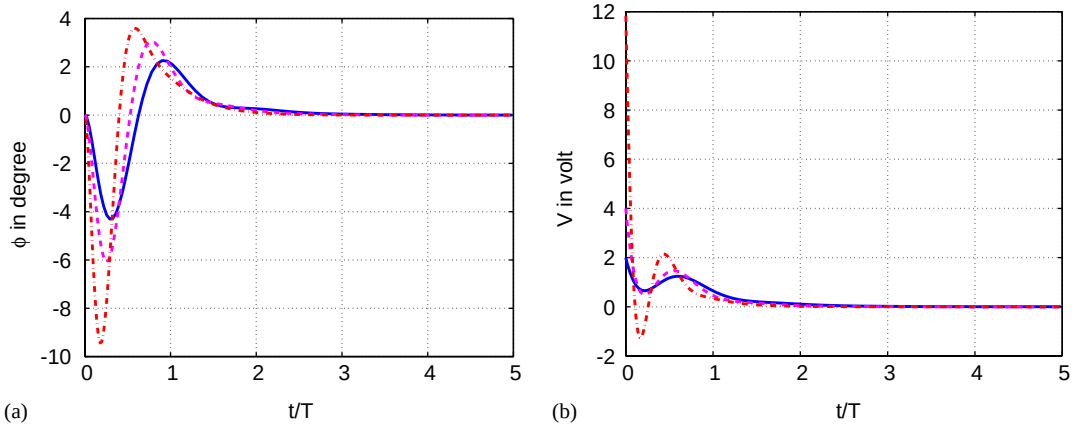

Fig. 9. Effect of changing K on the (a) load swing angle ϕ and (b) the control action using full-state feedback when $L = 1$ m and $m_t = 0$: ——, $K = 2$; - - -, $K = 4$; and - · - · - · -, $K = 12$.

the trolley equation, which affects the trolley acceleration and consequently the swing angle. Variation of K_ϕ with m_t can be considered a compensation for this force.

The effect of changing the load mass on the performance of the system is shown in Fig. 7. From inspection of the time histories, it is seen that the system response deteriorates if the gains are not adapted for the change in the load mass. An overshoot and hence an increase in the number of load oscillations occurs if the gains calculated for $m_t = 0$ were used when $m_t = 5$ because K_ϕ is larger than that required. We note a similar deterioration in the performance when the cable length is changed without adapting the gains, as shown in Fig. 8. The deterioration increases with

increasing cable length and load weight. However, the performance is more sensitive to variations in the cable length than to variations in the load mass. We note that, if the gains corresponding to a long cable were used to control the system with a shorter cable, there would not be an overshoot or an increase in the load oscillations. This is so because the used gain slows down the system more than required.

Variations of the feedback gains with cable length for $m_t = 0$ and the load mass for $L = 1$m using the full-state feedback controller are the same as those of the partial-state feedback controller. The results of implementing the full-state feedback controller for different values of K are shown in Fig. 9. The control action and the maximum swing angle decrease with decreasing K, while the response is slightly slower.

5. Experimental results

5.1. Friction estimation

To estimate the friction coefficients of the translational motion, we command the trolley to follow the reference signal

$$x_{\text{ref}} = 0.6\left[-0.4\sin\left(\frac{2\pi}{3}t\right) + 0.3\sin\left(\frac{2\pi}{4}t\right)\right]. \tag{34}$$

To stabilize the system, we use a PD controller. When we conducted the experiment using the tracking gains $K_p = 100$ and $K_d = 0.2$, we obtained two estimates for the friction coefficients. Comparing the outputs from several runs, we noted that the position and velocity differences are small. However, there is a large difference in the control actions. This is attributed to the magnification of the error caused by the high value of the controller gain K_p. To avoid this problem, we need to reduce K_p. A new set of gains is used: $K_p = 10$ and $K_d = 0.5$. Moreover, to avoid the problem arising from filtering the velocity, we use another set of gains: $K_d = 0$ and $K_p = 10$. The results of the estimation for different sets of gains are shown in Table 1. The cut-off frequency used is $\omega_c = 5$ Hz, whereas $d_s = 0.1$.

Examining these results, we note that the friction coefficients are nearly the same. These values are used as a starting guess for friction compensation. The final values obtained by fine-tuning are

$$\frac{b_+}{K_m} = 1.5, \qquad \frac{b_-}{K_m} = 6, \qquad \frac{c_+}{K_m} = 0.9, \qquad \frac{c_-}{K_m} = 1.2. \tag{35}$$

Table 1
Estimated friction coefficients for the translational motion

K_p	K_d	b_+/K_m	b_-/K_m	c_+/K_m	c_-/K_m
100	0.2	1.434	6.409	1.261	0.867
10	0.5	1.578	6.872	1.371	0.914
10	0	1.491	6.004	1.207	0.926

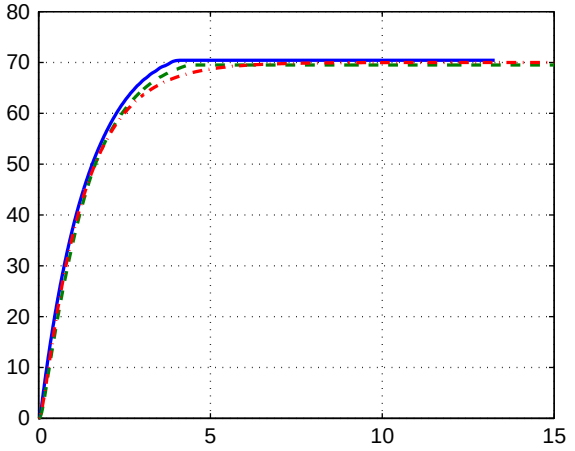

Fig. 10. The translational motion response to a step input with friction compensation: ——, positive direction; - - - -, negative direction; - · - · - · -, linear system.

To validate these results, we applied a step input to the trolley and the friction was compensated using the tuned coefficients. The response was compared with that of a linear frictionless model, Eq. (14). The controller gains were chosen to be $K_p = 6$ and $K_d = 1.33$. This comparison is displayed in Fig. 10, which shows that the friction compensation is acceptable. To complete the friction estimation, we determined the static friction from

$$\frac{fs_+}{K_m} \approx 1.0, \qquad \frac{fs_-}{K_m} \approx 1.2. \tag{36}$$

5.2. Gain-scheduling feedback controller

The values of the parameters which were used in the experiment are

$$K_{mx} = 2.0, \qquad m_t = 0.09, \qquad L = 1.0, \qquad T_s = 0.01\,\text{s}. \tag{37}$$

For $K_{mx} = 2.0$, the feedback gains for the translational motion are

$$K = \frac{3.8}{L}, \qquad K_{\dot{x}} = 1.33\sqrt{L}, \qquad K_{\phi} = L(3.9122 - 1.28925m_t). \tag{38}$$

The experimental results show the same behavior observed in the theoretical simulations. In the controlled case, the trolley reaches its destination nearly without overshoot while the load oscillates in only one cycle. Therefore, for the purpose of validations of our controller, we present only one case with $L = 1\,\text{m}$.

We started by placing the trolley at $x = 0.3\,\text{m}$ and then commanded it to move to $x = 0.75\,\text{m}$. Fig. 11 shows the response of the system with and without swing-angle feedback with the friction

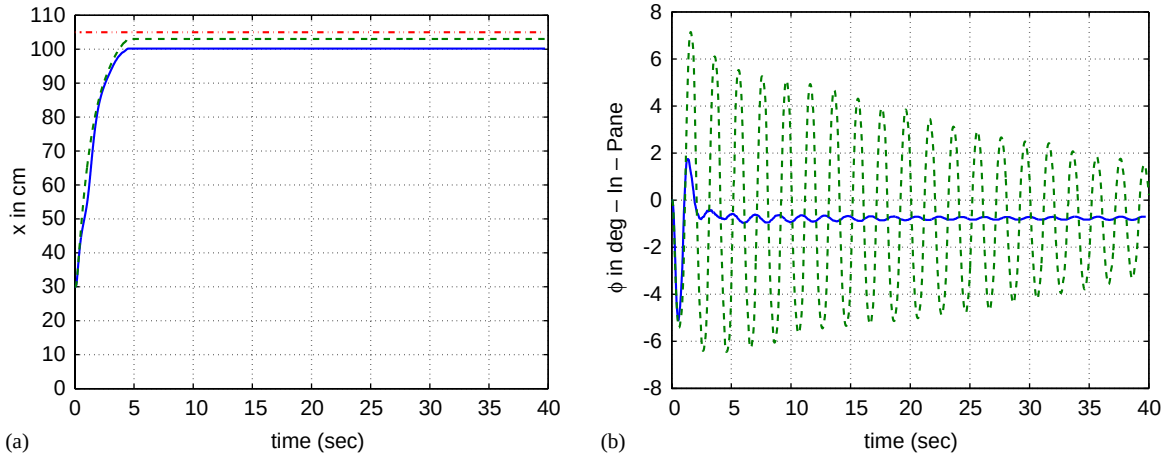

Fig. 11. Time histories of the translational motion when the trolley moves 0.75 m with and without swing-angle feedback. (a) Trolley position: ——, with friction compensation; - - - , without frictions compensation; - · - · - · - , set point X_{ref}. (b) Load swing: ——, with swing angle feedback; - - - , without swing angle feedback.

compensation being included in the control loop. Without the swing-angle feedback, the load swing was very high and took a long time to die out.

Fig. 12 shows the experimentally obtained response with and without friction compensation, with the swing-angle feedback being included. Without friction compensation, the trolley position had a high steady-state error. Also, the swing was small and was damped because of the slowness of the response, which resulted from the high frictional forces opposing the motion. With friction compensation, we note that the swing was suppressed; however, there was a steady-state error in the swing angle. This error resulted from an initial oscillation of the load. This error could be completely avoided if an absolute encoder rather than an incremental encoder was used. This error modifies the load destination point according to Eq. (39); that is,

$$X_{\text{ref}} = X_{\text{ref}} + K_{\phi}\phi_{\text{ss}}. \tag{39}$$

From the response in Fig. 12, $\phi_{\text{ss}} \approx -0.52^{\circ} = 0.00907$ rad, resulting in an actual set point of $X_{\text{ref}} = 1.014\,m$ instead of $X_{\text{ref}} = 1.05$. From this analysis, we conclude that the actual steady-state error of the trolley was 0.5 cm. This error was mainly due to the uncompensated friction. The residual swing oscillations in the swing angles are very small (0.15°) and they are hardly observed in reality. These oscillations are mainly due to the friction which could not be eliminated by the friction compensation. Sometimes, these oscillations could not be reduced to zero because the generated control action cannot reduced the residual friction. Therefore, the motion actuators could not move to compensate for these small swing angles. The magnitude of the residual swing angles depends on the state of the crane at which the actuator stuck. This state depends on the value of the friction as well as the dynamic of the motion. We also note that for the controlled case with friction compensation, the trolley reaches its final destinations without overshoot, while the load completes only one oscillation cycle at the end of the motion. The transfer time is nearly three times the load period, which is close to the optimal transfer time [5].

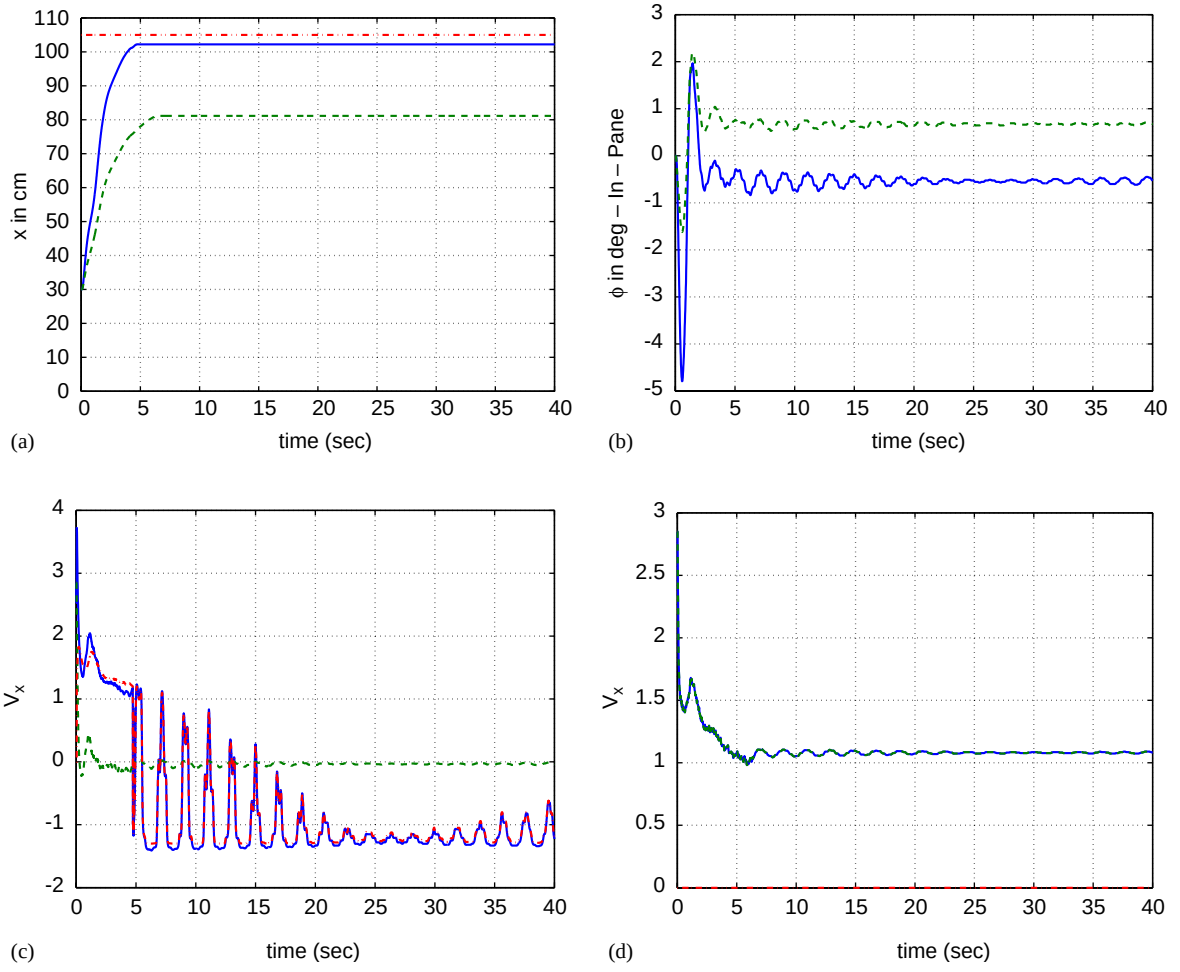

Fig. 12. Time histories of the translational motion when the trolley moves 0.75 m with and without friction compensation. (a) Trolley position: ——, with friction compensation; - - - , without frictions compensation; - · - · - · - , set point X_{ref}. (b) Load swing: ——, with friction compensation; - - - , without friction compensations. (c) Control action using friction compensation: - · - · - · -, linear system; - - -, friction compensation; ——, total. (d) Control action without friction compensation.

To investigate the effect of disturbances on the system, we started the crane from the rest position and then manually imparted it a disturbance. Fig. 13 shows the response of the system due to this disturbance with and without friction compensations. We note that the controller damped the load swing effectively when friction compensation was used.

6. Summary

State feedback is used to control the position and reduce the swing angle in gantry cranes for a wide range of cable lengths and load masses. The controller is closed loop, and hence it is suitable

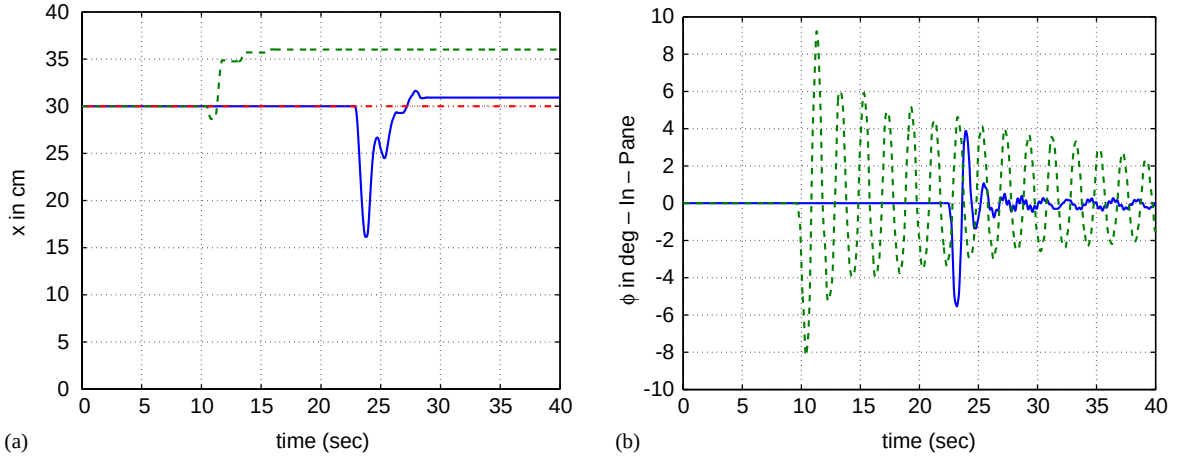

Fig. 13. Time histories of the translational motion when the trolley is subjected to a disturbance with and without friction compensation. (a) Trolley position: ——, with friction compensation; - - - , without frictions compensation; - · - · - · - , set point X_{ref}. (b) Load swing: ——, with friction compensation; - - - , without friction compensations.

for disturbance rejection and is insensitive to changes in the system parameters. The numerical simulations and the experimental results show that the controller is effective in reducing load oscillations and transferring the load in a reasonable time compared with that of optimal control. The friction compensation technique is an effective approach for reducing the effect of friction in mechanical systems. Moreover, control algorithms based on frictionless systems can be applied practically without modifications.

Acknowledgements

This work was supported by the Office of Naval Research (MURI) under Grant No. N00014-96-1123.

References

[1] P. Vaha, A. Pieska, E. Timonen, Robotization of an offshore crane, *Robots: Coming of Age*, *Proceedings of the 19th ISIR International Symposium*, 1988, pp. 637–648.

[2] Z. Masoud, A. Nayfeh, R. Henry, D. Mook, Cargo pendulation reduction on ship-mounted cranes via boom-luff and slew angles actuation, *Proceedings of the 41th Structures, Structural Dynamics, and Materials Conference*, Atlanta, GA, 2000.

[3] R.D. Robinett, G.G. Parker, J. Feddma, C. R. Dohrmann, J. Petterson, Sway control method and system for rotary crane, USA Patent No. 5908122, 1999 June.

[4] B. Balachandran, Y.Y. Lee, C.C. Fang, A mechanical filter concept for control of non-linear crane-load oscillation, *Journal of Sound and Vibration* 228 (3) (1999) 651–682.

[5] G.A. Manson, Time-optimal control of an overhead crane model, *Optimal Control Applications and Methods* 3 (1982) 115–120.

[6] B.L. Karihaloo, R.D. Parbery, Optimal control of dynamical system representing a gantry crane, *Journal of Optimization Theory and Applications* 36 (3) (1982) 409–417.

[7] Y. Sakaw, Y. Shindo, Optimal control of container cranes, *Proceedings of the Eighth IFAC Triennial World Congress on Control Science and Technology*, August, Kyoto, Japan, 1981, pp. 257–265.
[8] B.H. Karnopp, F.F. Fisher, B.O. Yoon, A strategy for moving a mass from one point to another, *Journal of the Franklin Institute* 329 (5) (1992) 881–892.
[9] C.L. Teo, C.J. Ong, M. Xu, Pulse input sequences for residual vibration reduction, *Journal of Sound and Vibration* 211(2) 157–177.
[10] W.E. Singhose, L.J. Porter, W. Seering, Input shaped of a planar gantry crane with hoisting, *Proceedings of the American Control Conference*, Albuquerque, NM, 1997, pp. 97–100.
[11] J.W. Besston, Closed-loop time optimal control of a suspended load, *Proceedings of the Fourth IFAC World Congress*, Warsaw, 1983, pp. 39–50.
[12] E. Ohnishi, I. Tsuboi, T. Egusa, M. Uesugi, Automatic control of overhead crane, *IFAC Eighth Triential World Congress*, 1981, pp. 1885–1890.
[13] A.J. Ridout, Anti-swing control of the overhead crane using linear feedback, *Journal of Electrical and Electronics Engineering* 9 (1/2) (1989) 17–26.
[14] A.J. Ridout, Variable damped control of the overhead crane, *IECON Proceedings, IEEE*, Vol. 2, Los Alamitos, CA, 1989, pp. 263–269.
[15] R. Salminen, A. Marttinen, J. Virkkunen, Adaptive pole placement control of a piloted crane, *Proceedings of the IFAC 11th Trienmal World Congress*, Tallinn, Estonia, 1990, pp. 313–318.
[16] A.D. Hazlergg, Automatic control of crane operations, *Proceedings of the Fifth IFAC World Congress*, Paris, 1972, pp. 11–13.
[17] R. Hurteau, R. Desantis, Microprocessor-based adaptive control of a crane system, *Proceedings of the 22nd IEEE Conference on Decision and Control, including The Symposium on Adaptive Processes*, Vol. 2, New York, 1983, pp. 944–947.
[18] H. Yang, Y. Kinouch, N. Sugio, Anti-swing fuzzy control of overhead cranes referring a velocity pattern, *Control and Cybernetics* 25 (2) (1996) 209–281.
[19] M.J. Nalley, M.B. Trabia, Design of a fuzzy logic controller for swing-damped transport of an overhead crane payload, *Dynamic Systems and Control* 1 (1994) 389–398.
[20] H. Lee, S. Cho, J. Cho, A new anti-swing control of overhead cranes, *IFAC Automation in the Industry*, Korea, 1997, pp. 115–120.
[21] O. Itho, H. Migita, Y. Irie, J. Itaho, Application of fuzzy control to automatic crane operation, *Japanese Journal of Fuzzy Theory and Systems* 6 (2) (1994) 283–296.
[22] A. Al-mousa, Tower Cranes Control using Fuzzy and Delay Controllers, MS Thesis, Virginia Tech, Blacksburg, VA, 2000.
[23] J.W. Auernig, H. Troger, Time optimal control of overhead cranes with hoisting of the load, *Automatica* 23 (4) (1987) 37–447.
[24] H.H. Lee, Modelling and control of a three-dimensional overhead crane, *Journal of Dynamic Systems, Measurement, and Control* 120 (1998) 471–476.
[25] H.M. Omar, A.H. Nayfeh, A simple adaptive feedback controller for tower cranes, *ASME 2001 Design Engineering Technical Conference and Computers and Information in Engineering Conference*, Pittsburgh, PA, September 9–12, 2001, DETC2001/VIB-21606.
[26] B. Armstrong, P. Dupont, C. Canudas, A survey of models, analysis tools, and compensation methods for the control of the machines with friction, *Automatica* 30 (70) (1994) 1083–1138.
[27] C. Canudas, *Adaptive Control for Partially Known Systems: Theory and Applications*, Elsevier, Amsterdam, Netherlands, 1988.
[28] C. Canudas, K.J. Astrom, K. Braun, Adaptive friction compensation in DC motor drives, *IEEE Conference on Decision and Control*, 1986, pp. 1556–1561.
[29] W. Li, X. Cheng, Adaptive high-precision control of positioning tables—theory and experiments, *IEEE Transactions on Control Systems Technology* 2 (3) (1994) 265–270.
[30] K.J. Astrom, B. Wittenmark, *Adaptive Control*, Addison-Wesley, Reading, MA, 1994.
[31] C. Canuda, H. Olsson, K.J. Astrom, A new model for control of systems with friction, *IEEE Transactions on Automatic Control* 40 (3) (1995) 419–425.